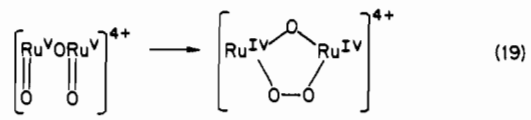

(19)

Such a pathway is not available to the trimer because of the O–Ru^{IV}–O "spacer" between the Ru–OH_2 sites.

The second is that the [V,V] dimer is sufficiently strong as an oxidant that it can carry out the net four-electron oxidation of H_2O to O_2 by a single intramolecular step or by a series of sequential intramolecular steps as shown by the thermodynamics of water oxidation[3] by [V,V] at pH 1:

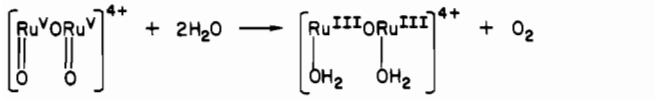

$E^{\circ\prime}$ = 0.25 eV (20)

Even though the oxidized forms of the trimer have the thermodynamic ability to oxidize water to oxygen, for one molecule of the trimer to oxidize water in a four-electron step, the trimer must be reduced at least to the [II,III,II] state. For the Ru–bpy trimer at pH 1, calculated $E^{\circ\prime}$ values for the five-electron couple [IV,IV,IV]/[II,III,II] and the six-electron couple [IV,V,IV]/[II,III,II] are 0.7 and 0.8 V vs. SCE, respectively. Thermodynamically, neither couple is capable of oxidizing water for which $E^{\circ\prime}$ = 0.93 V vs. SCE at pH 1.

Acknowledgment is made to X. B. Cox of this department for the measurement of XPS spectra. This research was supported by the National Institutes of Health under Grant No. 5-RO1-GM32296-02.

Registry No. $[Ru_3(bpy)_6O_2(OH_2)_2](ClO_4)_6$, 101954-90-9; $[Ru_3(bpy)_6O_2(OH_2)_2]^{9+}$, 101954-91-0; $[Ru_3(bpy)_6O_2(OH_2)_2]^{8+}$, 101954-92-1; $[Ru_3(bpy)_6O_2(OH_2)_2]^{5+}$, 101954-93-2; $[Ru_3(bpy)_6O_2(OH_2)_2]^{4+}$, 101695-59-4; $[Ru_3(bpy)_6O_2(OH_2)_2]^{3+}$, 101954-95-4; $[Ru_3(bpy)_6O_2(OH_2)_2]^{2+}$, 101954-94-3; $Ru(bpy)_2Cl_2$, 15746-57-3.

Contribution from the Department of Chemistry, The University of North Carolina, Chapel Hill, North Carolina 27514

Redox Properties of the Water Oxidation Catalyst $(bpy)_2(H_2O)RuORu(H_2O)(bpy)_2^{4+}$ in Thin Polymeric Films. Electrocatalytic Oxidation of Cl^- to Cl_2

William J. Vining and Thomas J. Meyer*

Received August 20, 1985

Chemically modified electrodes containing the ruthenium and osmium oxo-bridged dimers $[(bpy)_2(H_2O)M^{III}]_2O^{4+}$ (bpy = 2,2′-bipyridine) have been prepared by cation exchange into films of partially hydrolyzed *p*-chlorosulfonated polystyrene deposited onto glassy carbon electrodes. Both similarities and differences appear in comparing solution and film redox and acid–base properties: (1) As in solution the dimers undergo an initial one-electron oxidation, but the charge-transfer processes leading to higher oxidation states are inhibited in the polymeric film. (2) Reduction of the dimer leads to cleavage and formation of the monomers $(bpy)_2M(H_2O)_2^{2+}$ in the film. (3) In the film environment the dimers are less acidic than in solution. The catalytic oxidation of chloride ion by electrodes containing the Ru dimer has been studied in detail. Oxidation of a 1.0 M LiCl solution occurs with an initial current density of 100 mA/cm^2, and 26 000 turnovers/Ru site are obtained before deactivation of the catalyst occurs. Rotated-disk experiments show that the oxidation of Cl^- is independent of rotation rate but linearly dependent on $[Cl^-]$. Deactivation of catalyst appears to occur by oxidatively induced anation, possibly involving binding of sulfonate sites on the polymer to the dimer.

Introduction

Most of the work to date on the modification of electrode surfaces by the attachment of redox-active species either adsorbed or bound within an insoluble polymeric film has focused on simple electron-transfer processes.[1,2] A more demanding goal is the attachment of couples known to behave as redox catalysts in solution where, hopefully, some or all of the reactivity characteristics displayed in solution are retained in the environment of the polymeric film.

Redox reactions that occur by steps more complex than simple electron transfer are often beset with large overvoltages at electrode surfaces because of the inability of the electrode surface to meet the mechanistic demands of the reaction. Homogeneous redox catalysts have the advantage that they can be modified synthetically in a systematic fashion and detailed mechanistic studies can be carried out by using conventional techniques. If the reactivity characteristics of a solution catalyst can be maintained on an electrode surface or in a polymeric film, the possibility exists for developing electrode materials that operate with reactant specificity and decreased overvoltages. Some examples of redox catalysis based on surface-bound redox sites are known.[3-8]

Recently, it was shown that upon oxidation the μ-oxo-bridged Ru dimer $[Ru(bpy)_2(H_2O)]_2O^{4+}$ has the remarkable ability of catalyzing both the oxidation of water to dioxygen[9-11] and the oxidation of chloride to chlorine.[12] From the results of an electrochemical study it was concluded that oxidation of water may occur through a series of redox steps involving the loss of both protons and electrons with the final step being the loss of dioxygen and rebinding of two waters to the complex (eq 1, 2). Although the mechanistic details of the reaction are still under investigation, the key appears to be the final step where the highly oxidized Ru(V)–Ru(V) form of the dimer triggers the evolution of dioxygen. In addition, the Ru(V)–Ru(V) form of the dimer has been found to be a potent catalyst for the oxidation of Cl^- to Cl_2.

We report here on the redox and catalytic properties of the Ru dimer ion exchanged into the cation-exchange materials polystyrenesulfonate and Nafion. Our interest in the system was in comparing its reactivity properties in the polymeric film envi-

(1) Murray, R. W. *Acc. Chem. Res.* **1980**, *13*, 135.
(2) Murray, R. W. *Electroanal. Chem.* **1984**, *13*, 190.
(3) Calvert, J. M.; Meyer, T. J. *Inorg. Chem.* **1982**, *21*, 3978.
(4) Kutner, W.; Meyer, T. J.; Murray, R. W. *J. Electroanal. Chem. Interfacial Electrochem.* **1985**, *195*, 375.
(5) McHatton, R. C.; Anson, F. C. *Inorg. Chem.* **1984**, *23*, 3935.
(6) Buttry, D. A.; Anson, F. C. *J. Am. Chem. Soc.* **1984**, *106*, 59.
(7) Collman, J. P.; Marrocco, M.; Denisevich, P.; Koval, C.; Anson, F. C. *J. Electroanal. Chem. Interfacial Electrochem.* **1979**, *101*, 117.
(8) Samuels, G. J.; Meyer, T. J. *J. Am. Chem. Soc.* **1981**, *103*, 307.
(9) Gersten, S. W.; Samuels, G. J.; Meyer, T. J. *J. Am. Chem. Soc.* **1982**, *104*, 4029.
(10) Honda, K.; Frank, A. J. *J. Chem. Soc., Chem. Commun.* **1984**, 1635.
(11) Gilbert, J. A.; Eggleston, D. S.; Murphy, W. R.; Geselowitz, D. A.; Gersten, S. W.; Hodgson, D. J.; Meyer, T. J. *J. Am. Chem. Soc.* **1985**, *107*, 3855.
(12) (a) Ellis, C. D.; Gilbert, J. A.; Murphy, W. R.; Meyer, T. J. *J. Am. Chem. Soc.* **1983**, *105*, 4842. (b) Vining, W. J.; Meyer, T. J. *J. Electroanal. Chem. Interfacial Electrochem.* **1985**, *195*, 183–187.

0020-1669/86/1325-2023$01.50/0

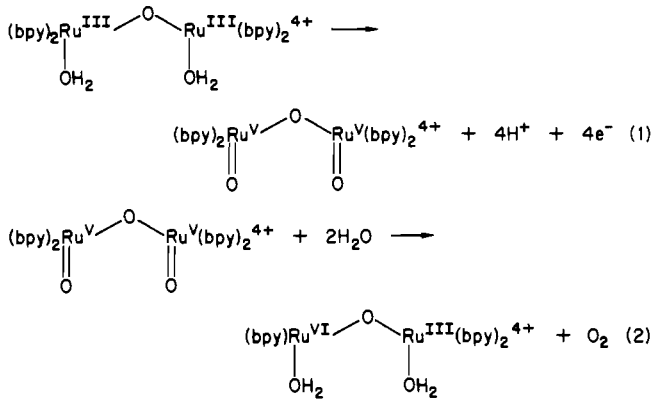

(1)

(2)

ronment with those in solution. Although electrodes with relatively low overvoltages toward oxidation of water and oxidation of chloride are known,[13-15] this is an important case in that it could provide a basis for inserting discrete chemical reaction sites into more complex film-based systems which could, for example, help provide a basis for artificial photosynthesis. Part of this work has appeared in a preliminary communication.[12b]

Experimental Section

Materials. All materials were reagent or ACS grade and were used as received unless otherwise noted. Buffer solutions at $\mu = 0.1$ M were prepared from perchloric acid/lithium perchlorate (pH 1–3), phosphoric acid/mono- and dibasic sodium phosphate (pH 4–9), sodium carbonate (pH 9–11), and sodium hydroxide/lithium perchlorate (pH 12–13).

The complexes $[[Ru(bpy)_2(H_2O)]_2O](ClO_4)_4$,[11] $[[Os(bpy)_2(H_2O)]_2O](ClO_4)_4$,[16] $[[Os(trpy)(bpy)]_2O](ClO_4)_4$,[17] and the trimer $[Ru_3(bpy)_6(\mu\text{-}O)_2(H_2O)_2](ClO_4)_4$[18] were prepared as described elsewhere. Polystyrene (M = 4000 and 10000) was purchased from Polysciences Corp.

Preparation of Chlorosulfonated Polystyrene. A solution of 1.0 g of polystyrene in 60 mL of CCl_4 was added dropwise to 35 mL of chlorosulfonic acid at 0 °C under an Ar atmosphere with stirring.[19] The reaction was quenched by pouring the reaction mixture onto ice and quickly filtering the resulting mixture. The product was washed with two 10-mL aliquots of ice-cold water, followed by copious amounts of benzene and dry ether. The degree of chlorosulfonation was determined by allowing 250 mg of the product to react with an excess of aniline, which undergoes sulfonamide condensation with the chlorosulfonyl group with release of chloride ion. The chloride ion content of the solution was determined by potentiometric titration with a standard solution of $AgNO_3$. The polymer samples in this study ranged between 50 and 90% chlorosulfonation based on the titrations.

Electrode Fabrication. Glassy carbon electrodes were fashioned from 3-mm carbon rods (Tokai) held in Teflon shrouds. The electrodes were polished with 1 μm diamond paste and dipped in a sonicator for 10 s prior to use. The electrode-coating procedure used was a drop coating method where a measured volume (1–10 μL) of an acetone solution with a known concentration of polymeric material was placed on the electrode surface. The surface tension of the acetone solution on the carbon disk was such that the entire carbon disk could be coated without coating the Teflon shroud, which allowed a known amount of polymeric material to be applied. Typically, 1×10^{-8} total equiv of chlorosulfonyl sites was deposited on the electrode surface.

Partial hydrolysis of the film was accomplished by immersing the electrodes in an aqueous solution at pH 9 for 15 min. The electrode was then washed gently with water and immersed in a solution of the complex being studied (at approximately 10^{-3} M) for 30–60 min. This was found to be the optimum soaking time for incorporation. Shorter times gave less incorporation while much longer times (>2 h) led to partial dissolution of the polymer (especially of the shorter chain length sample). The electrodes with complex incorporated were washed gently with water before use.

The reproducibility of electroactivity of the dimer-containing electrodes was studied systematically. For electrodes produced in an identical manner, the electroactivity in chloride-free solutions was quite reproducible with peak height variances of <10% for the first one-electron wave (see Results and Discussion) while the two-electron wave at more positive potentials varied up to 30%. However, there was a large variation in electrode activity toward catalytic oxidation of Cl^-. Typically, variations in activity of up to 50% were observed. Occasionally, an electrode was produced having a catalytic activity approximately 5 times that of the norm. These occurrences were rare (1 electrode out of 20), and their occurrence is as yet unexplained since every attempt was made to prepare the electrodes in an identical manner. The results of the systematic studies described below were based on measurements involving electrodes with "normal" activity.

Measurements

Cyclic voltammetry and controlled-potential electrolysis experiments were performed with a PAR Model 173 potentiostat/galvanostate and a PAR Model 175 universal programmer. All potential values reported are vs. the saturated sodium chloride calomel electrode (SSCE). $E_{1/2}$ values are the average of the reductive and oxidative peak potentials for the oxidative and reductive waves $(E_{pa} + E_{pc})/2$. A three-compartment electrochemical cell was used in all experiments to deter against contamination by small amounts of chloride ion. Coulometric measurements were made either by using a PAR Model 179 digital coulometer or by integrating the area under the current vs. time curves. Rotated-disk experiments were performed with the use of a Pine Model ASR rotator. Pulse polarographic experiments were carried out with a PAR Model 174a polarographic analyzer. Chronoamperometric experiments were performed by using a PAR Model 173 potentiostat/galvanostat equipped with a PAR Model 276 interface. The apparatus was interfaced with a PET 4032 microcomputer, which aquired and manipulated the data with programs written in-house. The potential was stepped approximately 200 mV past the peak of the wave studied, and the current–time profile was recorded (1000 points at 1 ms/point).

Results and Discussion

I. Preparation and Properties of Modified Electrodes. Electrode Preparation. The modification of glassy carbon electrodes by deposition of a film of *p*-chlorosulfonated polystyrene from an acetone solution has previously been reported.[19] The techniques used here are outlined in the Experimental Section. Immersing a film coated electrode in a weakly basic (pH 9–10 NaOH) solution for 15–30 min leads to partial hydrolysis of the chlorosulfonyl sites, yielding sulfonate sites (eq 3). Complete hydrolysis

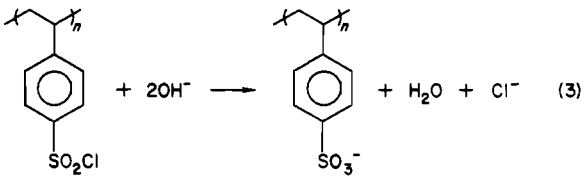

(3)

of the polymer does not occur under these conditions. Soaking a polymer that is approximately 40 units in length (M_r = 7000, ~90% chlorosulfonated) at pH 9–10 for longer periods (>10 h) leads to complete dissolution of the polymer. Longer chain length polymer samples (100 units) are less susceptible to dissolution. It should be noted that polystyrene sulfonate itself is soluble in aqueous solution at extremely high molecular weights (>100000).

In more strongly basic solutions (pH 13) dissolution of the shorter chain length polymer sample is far more rapid with complete dissolution occurring within minutes. For studies in strong base, only the long-chain-polymer samples were used and then only for relatively short times. The polymer is very stable with respect to dissolution in acidic solution with no discernible loss from the electrode over a period of 2 days. Our observations lead us to the conclusion that, under the conditions used in this study, the polymer is partially hydrolyzed to a mixed polymer containing some $-SO_2Cl$ sites, some $-SO_3^-$ sites, and possibly some cross-linked $-SO_2-O-SO_2-$ sites. Incorporation of the metal complexes into the hydrolyzed films was detailed in the Experimental Section.

(13) Denton, D. A.; Harrison, J. A.; Knowles, R. I. *Electrochim. Acta* **1979**, *24*(5), 521.
(14) Tilak, B. V. *J. Electrochem. Soc.* **1979**, *126*(8), 1343.
(15) Mills, A.; Zeeman, M. L. *J. Chem. Soc., Chem. Commun.* **1981**, 948.
(16) (a) Gilbert, J. A., Ph.D. Thesis, University of North Carolina at Chapel Hill, 1984. (b) Gilbert, J. A.; Geselowitz, D. A.; Meyer, T. J. *J. Am. Chem. Soc.* **1986**, *108*, 1493.
(17) Buckingham, D. A.; Dwyer, F. P.; Sargeson, A. M. *Aust. J. Chem.* **1964**, *17*, 622.
(18) Geselowitz, D.; Kutner, W.; Meyer, T. J. *Inorg. Chem.*, preceding paper in this issue.
(19) Ellis, C. D.; Meyer, T. J. *Inorg. Chem.* **1984**, *23*, 1748.

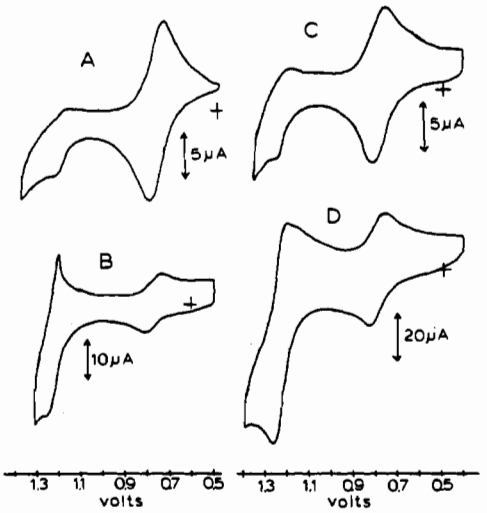

Figure 1. Cyclic voltammograms of $[(bpy)_2Ru(H_2O)]_2O^{4+}$ vs. SSCE incorporated within a partially hydrolyzed *p*-chlorosulfonated film (electrode I) in (A) 0.1 M $HClO_4$ and (C) 0.1 M HNO_3 and in (B) $HClO_4$ solution and (D) HNO_3 solution at a bare glassy carbon electrode (v = 50 mV/s). The traces are from single-sweep oxidative scans beginning at ~0.5 V.

Electrochemical Properties of Ru- and Os-Dimer-Modified Electrodes. Cyclic voltammograms of an electrode modified with partially hydrolyzed *p*-chlorosulfonated polystyrene/$[(bpy)_2Ru(H_2O)]_2O^{4+}$ (electrode I) in 0.1 M $HClO_4$ and in 0.1 M HNO_3 are shown in Figure 1, parts A and C, respectively. For comparison, cyclic voltammograms of the same complex in 0.1 M $HClO_4$ and in 0.1 M HNO_3 solution at a bare glassy carbon electrode are shown in Figure 1, parts B and D, respectively.[11] A number of similarities and dissimilarities between the film-bound and solution systems are immediately obvious. In all the voltammograms shown a reversible wave with $E_{1/2}$ = 0.79 V vs. SSCE attributed to the proton-coupled one-electron oxidation of the dimer (eq 4) is observed. Both in solution (Figure 1B,D) and in

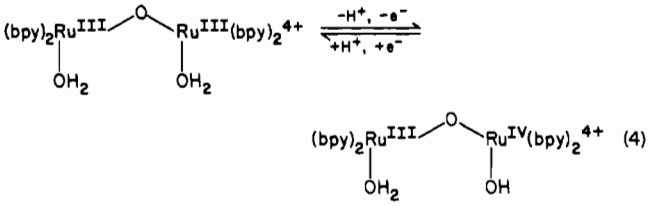

the film (Figure 1A,C) at a scan rate of 50 mV/s the splitting between the cathodic and anodic peaks of the couple is close to the theoretically predicted 59 mV for a reversible species diffusing to the electrode surface. At slower scan rates smaller peak splittings are observed for the polymer-bound species (35 mV at v = 10 mV/s), which is expected given the film-confined nature of the couple.

It is important to realize that our use of oxidation state labels like Ru(III)–Ru(IV) is merely a convenience. In fact, because of significant Ru–Ru interactions via $d\pi$(Ru)–$p\pi$(O)–$d\pi$(Ru) mixing, the mixed-valence ion may, in fact, be delocalized and be a more appropriate description $Ru^{III.5}Ru^{III.5}$.

In 0.1 M HNO_3 (Figure 1D) a wave at 1.2 V is observed arising from the proton-coupled three-electron oxidation of the $Ru^{III}Ru^{IV}$ form of the dimer (eq 5). At this pH in solution electrocatalytic

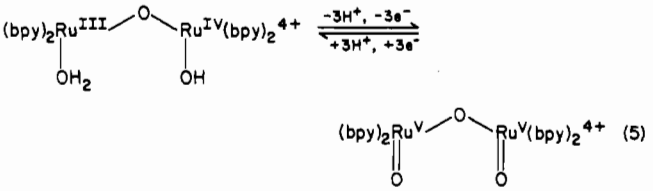

oxidation of water to oxygen by the dimer does occur but relatively

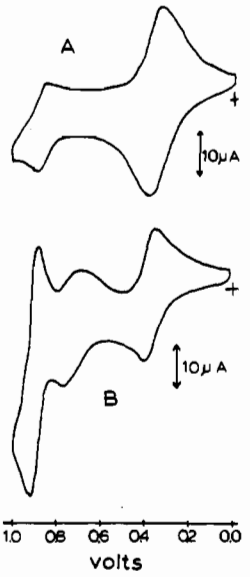

Figure 2. Cyclic voltammograms for $[(bpy)_2Os(H_2O)]_2O^{4+}$ vs. SSCE in (A) partially hydrolyzed *p*-chlorosulfonated polystyrene film on a glassy carbon electrode in 0.1 M $HClO_4$ and (B) in 0.1 M $HClO_4$ solution (~1 mM) at a bare glassy carbon electrode (v = 50 mV/s). The traces are from single-sweep oxidative scans starting at ~0.5 V.

slowly compared to the cyclic voltammetric scan rate.[11] It is interesting to note that at higher pH values, e.g. pH 4, distinct waves are observed for the two-electron III,IV/IV,V couple at $E_{1/2}$ = 1.02V (eq 6), followed by the one-electron IV,V/V,V couple

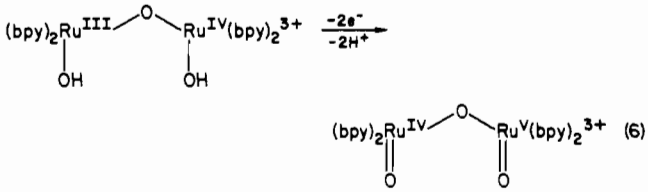

(eq 7). The appearance of a single three-electron wave at pH

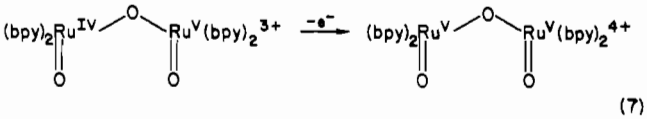

1 is a consequence of the difference in pH dependence of the two couples. Past pH 2.2, the potential for the III,IV/IV,V couple is *higher* than the potential for the IV,V/V,V couple, $(bpy)_2(O)Ru^{IV}ORu^{V}(O)(bpy)_2^{3+}$ is unstable with respect to disproportionation, and a single three-electron wave is observed. In 0.1 M $HClO_4$ solution (Figure 1B) the wave is misshapen due to electrode adsorption or precipitation.

The modified electrode (electrode I) shows drastically different properties for the higher couples. The three-electron wave at 1.2 V in 0.1 M HNO_3 is present but (Figure 1C) is smaller than the one-electron wave at 0.79 V and is unchanged by changing the medium to perchloric acid solution with no sign of an adsorption-like phenomenon. Oxidation of the Ru dimer to oxidation states higher than III,IV is kinetically hindered within the film and is probably a result of the inability of the complex to lose protons prior to electron transfer to the electrode. We were especially interested in the redox characteristics of the multiple-electron couple due to the catalytic abilities of the dimer in its higher oxidation states.

Modified electrodes were produced containing the osmium analogue of the ruthenium dimer. A cyclic voltammogram of an electrode prepared with partially hydrolyzed *p*-chlorosulfonated polystyrene and $[(bpy)_2Os(H_2O)]_2O^{4+}$ (electrode II) in 0.1 M $HClO_4$ is shown in Figure 2A. For comparison, a cyclic voltammogram of the osmium dimer in 0.1 M $HClO_4$ solution is

shown in Figure 2B.[16] The redox properties of the osmium dimer in solution mimic somewhat those of the ruthenium dimer with the redox potentials of the processes involved shifted to less negative potentials by approximately 400 mV. Consequently, the osmium dimer both in solution and in the film on an electrode surface displays an initial reversible redox wave with $E_{1/2}$ = 0.35 V vs. SSCE. This wave corresponds to the one-electron oxidation depicted in eq 8 at pH 1. At a scan rate of 50 mV/s the peak

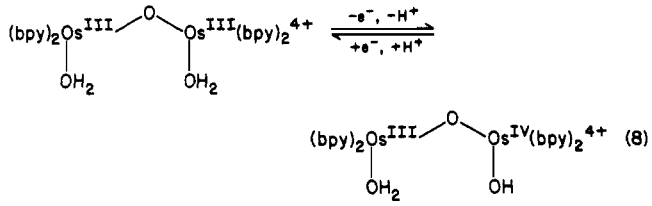

(8)

splitting for the first wave is 75 mV. As for the ruthenium complex, the properties of the one-electron process for the Os dimer are quite similar when in solution and when immobilized in the polymeric matrix.

Although three electron in character, further oxidation of the Os dimer differs in detail from that of the Ru dimer (eq 9a,b).

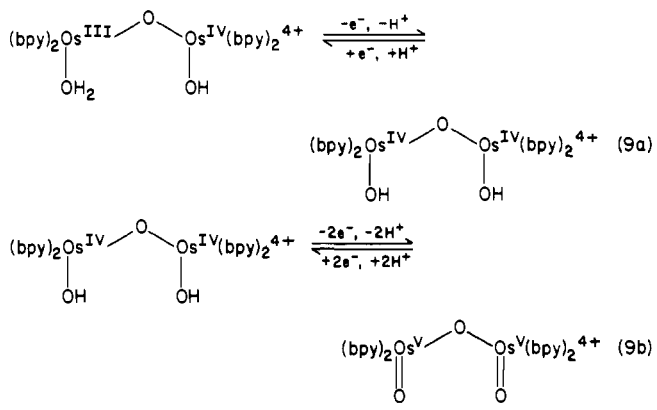

(9a)

(9b)

In acidic solution, the three-electron process for the Os dimer is split into successive one- and two-electron steps with Os(IV)–Os(IV) appearing as a stable intermediate oxidation state.

Oxidation past the Os(III)–Os(IV) dimer does not lead to the oxidation of water because, thermodynamically, Os(V)–Os(V) is not a sufficiently strong oxidizing agent. As a consequence, the Os dimer acts as a noncatalytic model for the intrinsic redox characteristics of the Ru dimer in the films.[16] The redox properties of the Os dimer in the polymeric films mimic those of the Ru dimer in that the total current for the multiple-electron processes at higher potentials is far less than expected on the basis of the current for the one-electron process (Figure 2a). Note that in the film only the two-electron process is observed and the peak splitting for the wave at a scan rate of 50 mV/s is 50 mV. This value, which is greater than the expected value of 30 mV for a diffusionally controlled two-electron process or 20 mV for a three-electron process, leads to the conclusion that, even for those dimeric sites that are capable of being oxidized past the III, IV stage, there are kinetic inhibitions to the oxidation and reduction processes.

pH Dependence of the Ru(IV)–Ru(III)/Ru(III)–Ru(III) Couple of the Ru-Dimer-Modified Electrodes. The redox couples observed for the Ru dimer in solution have a complex pH dependence due to the electron–proton-coupled nature of the net redox processes. We have studied the effect of pH on the redox properties of the modified electrode (electrode I). A plot of potential vs. pH for the one-electron III,III/III,IV wave is shown in Figure 3. There are five distinct regions in the plot, which are labeled a–e. they arise because of the acid–base properties of the two forms of the couple. From the experiments in solution, the couples in the various regions a–e are listed below (b = 2,2′-bipyridine). Although observed in solution, the acid-independent region a was not observed in the film. It is illustrated in Figure 3 by the dashed

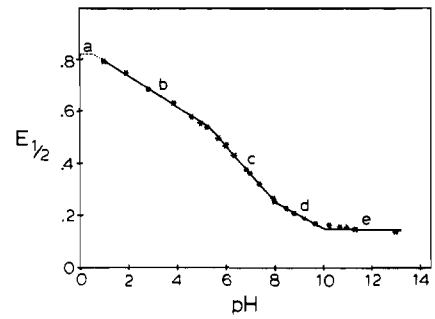

Figure 3. Plot of $E_{1/2}$ (vs. SSCE) for the $Ru^{III}Ru^{III}/Ru^{III}Ru^{IV}$ couple of electrode I vs. pH (values obtained at v = 50 mv/s).

Table I. Acid Dissociation Constants in Solution and within a Poly(styrenesulfonate) Film on a Glassy Carbon Electrode Surface (μ = 0.1 M; b = bpy)

acid	pK_a(film)[a]	pK_a(soln)[b]
$b_2Ru^{III}ORu^{IV}b_2^{5+}$ (OH$_2$, OH$_2$)		0.4
$b_2Ru^{III}ORu^{IV}b_2^{4+}$ (OH$_2$, OH)	5.3	3.2
$b_2Ru^{III}ORu^{III}b_2^{4+}$ (OH$_2$, OH$_2$)	8.2	5.9
$b_2Ru^{III}ORu^{III}b_2^{3+}$ (OH$_2$, OH)	9.9	8.3

[a] Buffer solutions used as described in the Experimental Section at ambient temperature. [b] Solution values from ref 11.

line, assuming that for $(bpy)_2(H_2O)Ru^{III}ORu^{IV}(H_2O)(bpy)_2^{5+}$ pK_{a_1} = 0.4, the value in solution.

region couple

a $b_2Ru^{III}ORu^{IV}b_2^{5+} + e^- \rightarrow b_2Ru^{III}ORu^{III}b_2^{4+}$ (OH$_2$, OH$_2$ → OH$_2$, OH$_2$)

b $b_2Ru^{III}ORu^{IV}b_2^{4+} + e^- + H^+ \rightarrow b_2Ru^{III}ORu^{III}b_2^{4+}$ (OH$_2$, OH → OH$_2$, OH$_2$)

c $b_2Ru^{III}ORu^{IV}b_2^{3+} + e^- + 2H^+ \rightarrow b_2Ru^{III}ORu^{III}b_2^{4+}$ (OH, OH → OH$_2$, OH$_2$)

d $b_2Ru^{III}ORu^{IV}b_2^{3+} + e^- + H^+ \rightarrow b_2Ru^{III}ORu^{III}b_2^{3+}$ (OH, OH → OH, OH$_2$)

e $b_2Ru^{III}ORu^{IV}b_2^{3+} + e^- \rightarrow b_2Ru^{III}ORu^{III}b_2^{2+}$ (OH, OH → OH, OH)

The breaks in the plot correspond to changes in the proton content of either the III,III or III,IV forms of the dimer, which allow pK_a values for the different forms of the dimer to be estimated from the breaks in its pH–potential plots. In Table I are listed pK_a values for the different forms of the dimer both in solution[11] and in the derivatized polystyrene film on the electrode. It is interesting to note that in all cases pK_a values are noticeably greater in the film environment and the acidity is less than in solution. The decrease in acidity is notable and is probably a consequence of the polyanionic environment within the film, which would tend to stabilize the more highly charged, acidic forms of the acid–base pair.

The shapes of the voltammograms are also affected by changes in pH. Figure 4 shows a cyclic voltammogram of electrode I in a solution buffered at pH 7. Note that at this pH, and above pH 2.2 in general, the couple at higher potential is the two-electron III,IV/IV,V couple. In contrast to the behavior in Figure 1, the

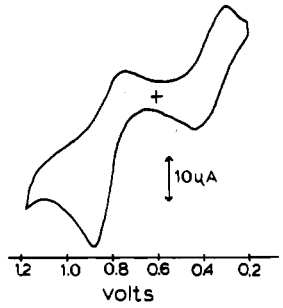

Figure 4. Cyclic voltammogram of electrode I in pH 7 phosphate-buffered solution (v = 50 mV/s) from a single-sweep oxidative scan vs. SSCE.

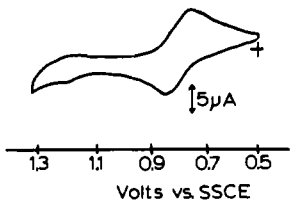

Figure 5. Cyclic voltammogram of $[(bpy)_2Ru(H_2O)]_2O^{4+}$ incorporated into a 1200 equiv wt Nafion film on a glassy carbon electrode in 0.10 M $HClO_4$ (v = 50 mV/s) from a single-sweep oxidative scan vs. SSCE.

oxidative component of the two-electron wave (at 0.88 V) is approximately twice the size of the one-electron wave (at 0.46 V) although the current for the reductive component remains suppressed. As a general rule, couples within the polymeric films display behavior more closely resembling that of solution couples at pH >5. The dramatic decrease in current for the multiple-electron wave occurs only in solutions at pH <5.

Medium Effects on the Electrochemical Properties of Ru-Dimer-Modified Electrodes. The effects of changing the ionic medium on the redox properties of the dimer within polysulfonate films (electrode I) were studied. No significant differences were observed with the use of different acids ($HClO_4$, HNO_3, H_2SO_4, or HCl for the lower potential wave although catalytic oxidation of chloride occurs at higher potentials). The addition of supporting electrolytes with differing cations ($[NEt_4]ClO_4$, $LiClO_4$, $NaClO_4$) also showed no effect. No obvious differences were observed when different samples of chlorosulfonated polystyrene were used. Samples with differing degrees of chlorosulfonation (50–90%) and differing chain lengths (40 and 100 units) only affected the degree of loading of the metal complex into the polymer and the solubility of the polymer in basic solution.

The electrochemistry of the Ru dimer in the perfluorinated polymer Nafion

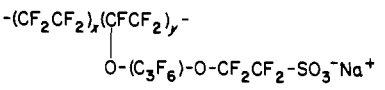

was also studied.[20] A cyclic voltammogram of a glassy carbon electrode coated with Nafion and loaded with $[(bpy)_2Ru(H_2O)]_2O^{4+}$ in 0.1 M $HClO_4$ is shown in Figure 5. Note that the voltammogram closely resembles that of the complex in the polystyrene sulfonate matrix with the prominent feature being the apparent loss of current for the three-electron wave at 1.2 V. Similar results have been observed for the Ru dimer ionically bound to Dowex beads in carbon paste.[21]

Stability of the Ru Dimer within the Polymeric Film. The electrochemical stability of the electrodes modified with the Ru dimer (electrode I) was investigated. In 0.1 M $HClO_4$, continued cycling through the one-electron wave (0.5–1.0 V) resulted in a slow decrease in peak current ($t_{1/2}$ = 30 min). The loss of current was unaffected by holding the potential at 0.5 or 0.9 V, that is, by keeping the complex in the III,III or III,IV forms. Note that

(20) Nafion is a registered trademark of E. I. duPont de Nemours & Co.
(21) Kutner, W., personal communication.

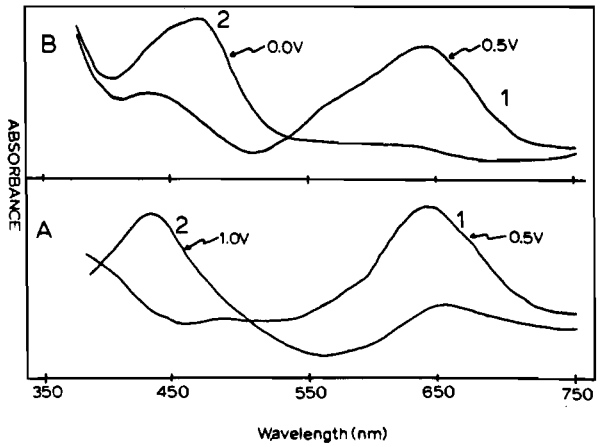

Figure 6. Visible spectra of $[(bpy)_2Ru(H_2O)]_2O^{4+}$ incorporated into a Nafion film on an SnO_2 optically transparent electrode in 0.1 M $HClO_4$: A, (1) with electrode potential held at 0.5 V and (2) after holding the potential of the electrode at 1.0 V for 30 min; B, (1) with the electrode potential held at 0.5 V and (2) after holding the potential of the electrode at 0.0 V for 20 min.

at pH 1 the overall charge on the dimer in either oxidation state remains +4. If the electrode was resoaked in a dimer-containing solution for 15 min, the electroactivity was fully restored. Since the polymer itself is stable on the electrode for long periods of time in this medium, it is clear that the loss of current is due to leaching of the complex from the film into the bulk solution.

Cycling through both waves (0.5–1.35 V) results in a relatively rapid loss of current in both waves with a new wave appearing at about 0.6 V. Although yet to be properly documented, the process observed is probably oxidatively induced anation, as can be seen for the dimer in solutions containing Cl^-, SO_4^{2-}, or NO_3^-.[16a] The product at 0.6 V may well arise from a dimer containing a bound sulfonate group from the polymeric backbone although anation by the anion of the supporting electrolyte is also possible. The apparent "anation" process is reversible. Resoaking the electrode in an aqueous solution results in partial reaquation of the complex while soaking in a dimer-containing solution results in the full restoration of electroactivity as mentioned above.

In weakly basic solution (pH 9) the complex is stable toward cycling through both waves with little anation observed although loss of the dimer from the film still occurs. In strong base (0.1 M NaOH) the main destabilizing effect is dissolution of the polymer. Loss of polymer is in keeping with the fact that the chlorosulfonyl sites in the polymer hydrolyze at a faster rate in more basic solutions and dissolution is a direct outcome of extensive hydrolysis. Short-chain polymers (40 units) dissolve quickly, and little electrochemical response was observed. Longer chain polymers (100 units), however, show an interesting effect. Cycling through either the first or both waves leads to peak current increases for about six cycles and then decreases over about ten cycles until electroactivity is completely lost. The initial enhancement may arise because of hydrolysis of additional chlorosulfonated sites, leading to an opening of the polymer film (swelling), allowing far more rapid charge transport. The loss mechanism is by dissolution of the polymer as discussed above, and careful examination of the electrode surface at the end of the electrochemical experiment shows no polymer remaining on the surface.

The spectral characteristics of the various forms of the Ru dimer in the polymeric films have been studied to help discern the state of the complex in the ion-exchange environment. Figure 6a shows the spectrum of $[(bpy)_2Ru(H_2O)]_2O^{4+}$ when bound within a Nafion film on an SnO_2 optically transparent electrode. Spectrum 1 is of the dimer in the III,III state. The band maximum is at 644 nm, which is quite close to the solution maximum in acid solution at 637 nm. Spectrum 2 is of the film after electrolyzing in a pH 1 solution at 0.95 V for 30 min. At this potential the dimer is oxidized by one electron to the III,IV state. The spectrum has a maximum at 430 nm, which is similar to the value of 444

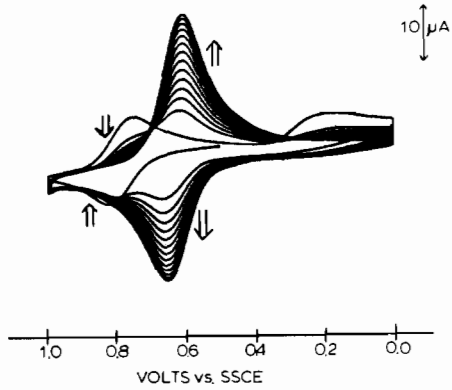

Figure 7. Cyclic voltammogram of electrode I between 0.0 and 1.0 V in 0.1 M $HClO_4$. Arrows denote disappearance of $[(bpy)_2Ru(H_2O)]_2O^{4+}$ and appearance of *cis*-$(bpy)_2Ru(H_2O)_2^{2+}$; v = 20 mV/s.

nm for the dimer at pH 0, where the dominant form is the diaquo dimer $[(bpy)_2Ru(H_2O)]_2O^{5+}$. Note that spectrum 2A shows some dimer remaining in the blue, III,III form. The inability of all of the III,III sites to be oxidized further supports the cyclic voltammetric results, which indicate that some of the complex is electrochemically inactive. Since the absorption spectrum of the unreacted sites is unchanged, they must be trapped in pockets within the film that render them inactive toward oxidation.

In solution, the first pK_a for the diaquo III,IV dimer is 0.4. It is interesting to note that, at pH 1, λ_{max} for the III,IV dimer is at 495 nm since, at this pH, the dominant form of the dimer is $(bpy)_2(H_2O)Ru^{III}ORu^{IV}(OH)(bpy)_2^{4+}$. By inference, the decrease in acidity within the polymeric film for the III,III and III,IV dimers noted in Table I must also carry over to the first pK_a for the III,IV dimer and pK_{a1} within the film must be less than 1.0.

Reductive Cleavage of $[(bpy)_2Ru(H_2O)]_2O^{4+}$ to $(bpy)_2Ru(H_2O)_2^{2+}$. Figure 7 shows the effect of scanning the Ru dimer modified electrode reductively to 0.0 V in 0.1 M $HClO_4$. Note the irreversible wave at E_p = 0.23 V which, by comparison with the known chemistry in solution, arises from the reduction of the III,III dimer to an unstable II,III form. The reductive scans lead to loss of current for the one-electron, dimer-based wave at 0.79 V with concomitant growth of a wave with $E_{1/2}$ = 0.63 V. The behavior in the film is analogous to that observed in solution where initial reduction of the dimer by one electron in acidic solution leads to cleavage of the Ru–O–Ru link and formation of two molecules of *cis*-$(bpy)_2Ru(H_2O)_2^{2+}$ (eq 10).[11]

$$[(bpy)_2Ru(H_2O)]_2O^{4+} + 2e^- + 2H^+ + H_2O \rightarrow 2cis\text{-}(bpy)_2Ru^{II}(H_2O)_2^{2+} \quad (10)$$

The wave at 0.63 V corresponds to the proton-coupled one-electron oxidation of the Ru monomer from Ru(II) to Ru(III) (eq 11).

$$cis\text{-}(bpy)_2Ru^{II}(H_2O)_2^{2+} \underset{+e^-,\,+H^+}{\overset{-e^-,\,-H^+}{\rightleftharpoons}} cis\text{-}(bpy)_2Ru^{III}(H_2O)(OH)^{2+} \quad (11)$$

An analysis of the reactant and product voltammograms reveals an interesting fact. The area under the product wave at 0.63 V is approximately 4–5 times greater than that under the reactant wave at 0.79 V (the actual value varies somewhat from one electrode to another). By contrast, the stoichiometry of eq 10 leads to the prediction of a ratio of products to reactant of 2. The enhanced current for the monomer clearly shows that there are oxidatively inactive dimeric molecules within the polymeric film that become redox active when converted into the monomer. Similar results have been reported for $Ru(bpy)_3^{2+}$ incorporated into Nafion coatings[22] and for $-Fe(CN)_5^{3-}$ incorporated into poly(vinylpyridine) coatings.[23]

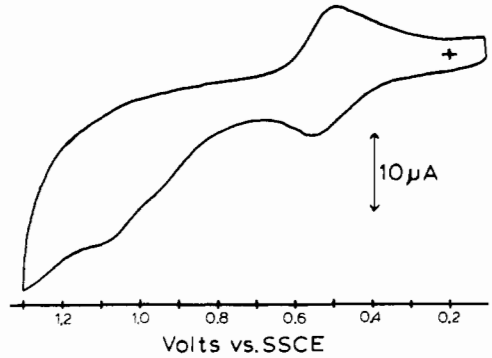

Figure 8. Cyclic voltammogram of *cis*-$(bpy)_2Ru(H_2O)_2^{2+}$ incorporated into a partially hydrolyzed *p*-chlorosulfonated polystyrene film on a glassy carbon electrode in pH 4.01 buffer (v = 50 mV/s).

The reductive cleavage of the dimer was also studied spectrophotometrically. Figure 6B shows a spectrum of the Ru dimer in Nafion before (spectrum 1) and after (spectrum 2) electrolysis at 0.0 V for 20 min. Spectrum 1 shows that the dimer is partially in the III,IV form. Spectrum 2 shows the virtual disappearance of the band at 639 nm with the appearance of a band at 468 nm, consistent with the appearance of $(bpy)_2Ru(H_2O)_2^{2+}$ in pH 1 solution.[24]

The same reductive cleavage chemistry is observed for the Os dimer in solution and on the modified electrode. Thus, scanning an electrode modified with the Os dimer (electrode II) between −0.5 and +0.5 V in 0.1 M $HClO_4$ results in diminution of the wave for the dimer at 0.35 V concurrent with growth of a wave at 0.14 V due to oxidation of *cis*-$(bpy)_2Os(H_2O)_2^{2+}$ to Os(III).[25] Interestingly, a comparison of the peak areas shows that the integrated Os(III),Os(II) wave is only 1.8 times that for the dimer, suggesting that in contrast to the Ru case there is no charge-transfer rate advantage for the Os monomer over the Os dimer. We have also investigated in the same type of experiment the Ru trimer $(bpy)_2(H_2O)RuORu(bpy)_2ORu(H_2O)(bpy)_2^{4+}$. In acidic solution the trimer displays a one-electron oxidation at 1.16 V and, in addition, an irreversible reduction that leads to cleavage of the Ru–O–Ru linkages to form three monomeric fragments (eq 12).[18] Modified electrodes containing the trimer were reduced

$$2H_2O + 4H^+ + 2e^- + Ru_3(bpy)_6(O)_2(OH_2)_2^{4+} \rightarrow 2cis\text{-}(bpy)_2Ru^{II}(H_2O)_2^{2+} + trans\text{-}(bpy)_2Ru^{II}(H_2O)_2^{2+} \quad (12)$$

at 0.0 V with the formation of one trans and two cis monomeric fragments. The redox potential for the Ru(III)/Ru(II) couple of *trans*-$(bpy)_2Ru(H_2O)_2^{2+}$ is 0.44 V and overlaps with the wave for *cis*-$(bpy)_2Ru(H_2O)_2^{2+}$ at 0.63 V. The area under the combined waves for the two monomeric species was approximately 14 times that under the one-electron wave at 1.16 V for the trimer. From the results on these systems it is clear that the polymeric film environment has a significant impact on the charge-transport properties of related monomers and oligomers and selectivity effects can depend intimately on the nature of the species involved.

Electrochemical Properties of Monomer-Containing Modified Electrodes. Figure 8 shows a cyclic voltammogram for a modified electrode containing *cis*-$(bpy)_2Ru(H_2O)_2^{2+}$ in 0.1 M $HClO_4$ solution. In contrast to the case of the dimer, the electrochemical characteristics of the monomer in the film correlate well with those in solution. Both the Ru and Os monomers undergo a series of proton-coupled redox reactions (eq 13–16).[25]

(22) Martin, C. R.; Rubinstein, I.; Bard, A. J. *J. Am. Chem. Soc.* **1982**, *104*, 4817.

(23) Kiyotaka, S.; Noboru, O.; Anson, F. C. *J. Am. Chem. Soc.* **1981**, *103*, 2552.

(24) Durham, D.; Wilson, S. R.; Hodgson, D. J.; Meyer, T. J. *J. Am. Chem. Soc.* **1980**, *102*, 600.

(25) (a) Takeuchi, K. J.; Samuels, G. J.; Gersten, S. W.; Gilbert, J. A.; Meyer, T. J. *Inorg. Chem.* **1983**, *22*, 1407. (b) Dobson, J.; Pipes, D. W.; Meyer, T. J. *Inorg. Chem.*, in press. (c) Dobson, J., work in progress.

$$cis\text{-}(bpy)_2M^{II}(H_2O)_2^{2+} \xrightarrow{-e^-,\,-H^+} cis\text{-}(bpy)_2M^{III}(H_2O)(OH)^{2+} \quad (13)$$

$$cis\text{-}(bpy)_2M^{III}(H_2O)(OH)^{2+} \xrightarrow{-e^-,\,-H^+} cis\text{-}(bpy)_2M^{IV}(O)(H_2O)^{2+} \quad (14)$$

$$cis\text{-}(bpy)_2M^{IV}(O)(H_2O)^{2+} \xrightarrow{-e^-,\,-H^+} cis\text{-}(bpy)_2M^{V}(O)(OH)^{2+} \quad (15)$$

$$cis\text{-}(bpy)_2M^{V}(O)(OH)^{2+} \xrightarrow{-e^-,\,-H^+} cis\text{-}(bpy)_2M^{VI}(O)_2^{2+} \quad (16)$$

We have investigated the stability of the monomeric complexes within the film. Recent work has shown that the Os(VI) dioxo complex *cis*-$(bpy)_2Os(O)_2^{2+}$ undergoes the irreversible loss of a bipyridine ligand in acidic solution, giving *trans*-$(bpy)Os(O)_2(OH)_2^{2+}$.[25b]

Holding the potential of a modified electrode containing $(bpy)_2Os(H_2O)_2^{2+}$ at 1.0 V (causing formation of Os(VI)) results in a chemical transformation with a concurrent change in the electroactivity of the electrode. Figure 9A shows a cyclic voltammogram of such an electrode after the potential was held at 1.0 V for 10 min. The electrochemistry of the monobipyridine complex in the film is similar to that of the corresponding phenanthroline complex in solution.[25b,26] We also find that similar bpy loss occurs for the corresponding Ru(VI) monomer, $(bpy)_2Ru(H_2O)_2^{2+}$. Figure 9B shows a cyclic voltammogram for an electrode modified with the Ru monomer after it was held at a potential of 1.3 V for 10 min. Parts A and B of Figure 9 are remarkably similar in appearance with the only significant difference between the corresponding Ru and Os complexes being the expected shift to lower potentials for Os relative to Ru.

Electrode Kinetics. A series of measurements were undertaken to explore the kinetic aspects of the charge-transfer processes within the film for the various film-coated electrodes. The dependence of oxidative peak current, i_{pc}, on scan rate, v, was studied for modified electrodes containing both dimers and monomers of Ru and Os. Figure 10 shows a plot of ln i_{pc} vs. ln v for the III, IV/III,III couple of an electrode containing the Ru dimer (electrode I) in 0.1 M HNO_3. The slope of the plot gives an indication of the diffusional nature of the redox process under investigation. A slope of 0.5 indicates semiinfinite diffusional behavior (i.e. $i_p \propto v^{1/2}$) while a slope of 1.0 indicates finite diffusion kinetics in the thin-layer regine (i.e. $i_p \propto v$).

For the Ru dimer a plot of ln i_p vs. ln v is linear with a slope of 0.71 ± 0.01 indicating partially diffusional behavior. The same electrode in 0.1 M $HClO_4$ gave a slope of 0.69 ± 0.02. For comparative purposes, the i_{pc} vs. v dependence for electrodes containing the oxo-bridged dimer $[(bpy)(trpy)Os]_2O^{4+}$ was also investigated. This dimer is approximately the same size and charge type as the aqua dimers but has a reversible, proton-independent, one-electron redox couple at $E_{1/2}$ = 0.68 V corresponding to oxidation to the Os(III)Os(IV), +5 dimer $[(bpy)(trpy)Os]_2O^{5+}$. For the trpy–bpy dimer a plot of ln i_p vs. ln v gave a slope of 0.48 ± 0.02 and, of all the electrodes studied, showed the most solution-like behavior.

Data for the charge-transfer kinetics of the monomeric and dimeric aquo systems are listed in Table II. All of the aqua complexes studied show behavior that is only partially semidiffusional, and it seems clear that the proton-coupled nature of the aqua complex redox processes inhibits charge transfer through the film. It is important to note, also, that although the Ru monomer displays greater electroactivity within the film than the corresponding dimer, both processes seem to be equally diffusional in character.

The effect of scan rate variations on the potential difference between the cathodic and anodic peak currents of the voltammograms, which gives an indication of the rate of charge transfer, was also studied for the modified electrodes. For an ideal surface-bound couple where there is no diffusional component to the charge-transfer event and heterogeneous charge transfer is rapid, ΔE_p is predicted to be 0. Figure 11 shows a plot of ΔE_p vs. v for the one-electron wave for electrode I in 0.1 M $HClO_4$. At fast

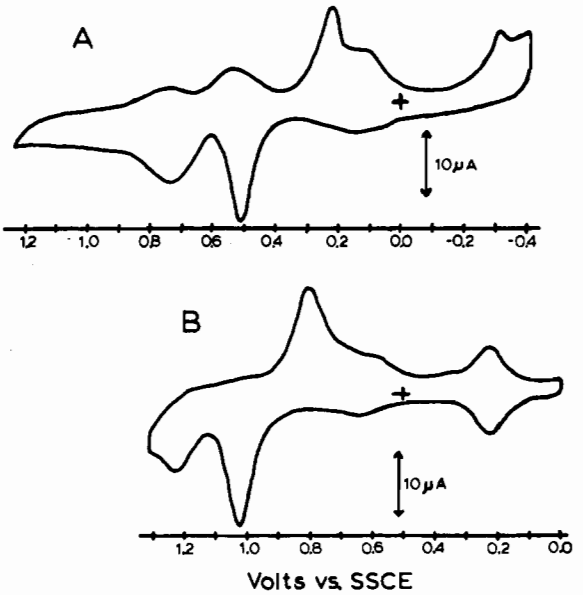

Figure 9. (A) Cyclic voltammograms of a modified electrode containing $(bpy)_2Os(H_2O)_2^{2+}$ after holding the potential at 1.0 V for 10 min in 0.10 M $HClO_4$ (v = 50 mV/s). (B) Cyclic voltammogram of a modified electrode containing $(bpy)_2Ru(H_2O)_2^{2+}$ after holding the potential at 1.3 V for 10 min in 0.10 M $HClO_4$ (v = 50 mV/s).

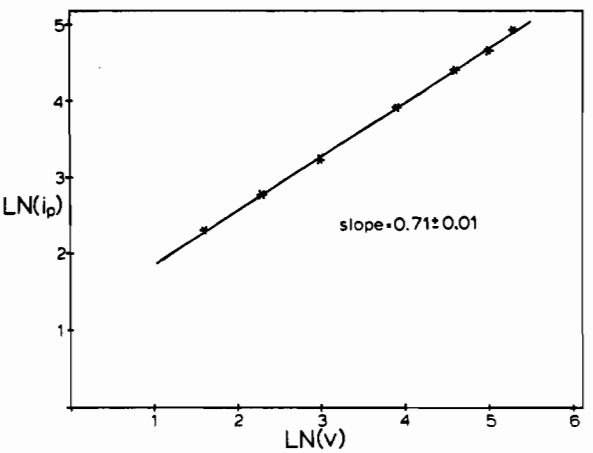

Figure 10. Plot of ln i_p vs. ln v for electrode I in 0.10 M HNO_3; i_p obtained from peak of cyclic voltammogram with substracted background currents.

Table II. Electrochemical Kinetics Data for Various Complexes Bound within a Chlorosulfonated Polystyrene–Poly(styrenesulfonate) Film on Glassy Carbon Electrodes[a]

complex	$10^9 D_{ct}C$[b]	$10^9\Gamma$,[c] mol	C, M	$10^9 D_{ct}$, $cm^2\ s^{-1}$
$[[(bpy)_2Ru(H_2O)]_2O](ClO_4)_4$	2.57	1.94	0.22	11.2
$[(bpy)_2Ru(H_2O)_2](ClO_4)_2$	4.52	3.63	0.42	10.5
$[[(bpy)_2Os(H_2O)]_2O](ClO_4)_4$	2.08	2.65	0.31	6.67
$[(bpy)_2Os(H_2O)_2](ClO_4)_2$	3.07	4.18	0.49	6.24

[a] Data obtained in 0.1 M $HClO_4$ at ambient temperature. The diffusion coefficient for charge transfer, D_{CT}, the surface coverage of redox sites, Γ, and the concentration of redox sites within the films, C, are defined in more detail in the text. [b] Obtained from chronoamperometric measurements; ±5%. [c] Total amount of electroactive material on the electrode as determined by integration of cyclic voltammetric curves.

(26) Galas, A. M. R.; Hursthouse, M. B.; Behmann, E. J.; Midden, W. R.; Green, G.; Griffith, W. P. *Transition Met. Chem. (Weinheim, Ger.)* **1981**, *6*, 194.

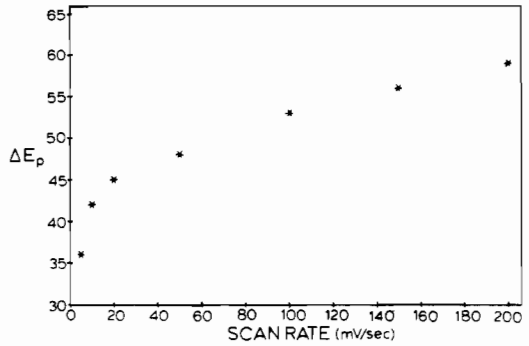

Figure 11. Plot of $E_{pa} - E_{pc}$ for electrode I in 0.10 M $HClO_4$ vs. scan rate, v.

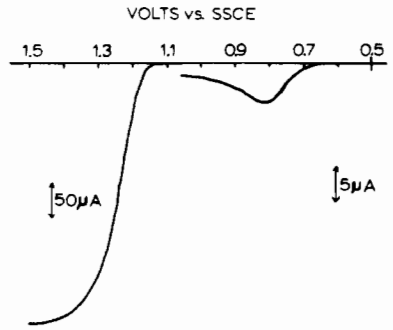

Figure 12. Rotated-disk voltammogram of electrode I in 0.10 M $HClO_4$ containing 0.10M LiCl (ω = 1600 rpm; v = 10 mV/s). The wave at ~0.8 V is for the III,IV/III,III couple. The background current without catalyst is less than 5% of that shown with catalyst.

scan rates (v > 50 mv/s) solution-like behavior is observed with $\Delta E_p \rightarrow 60$ mV while at slower scan rates (v < 20 mV/s) the ΔE_p values decrease with decreasing v and fall as low as 35 mV (at v = 5 mV/s). It should be noted that some dimer-containing electrodes display ΔE_p values as high as 75 mV at scan rates above 50 mV/s. This and the preceding information reinforce the earlier conclusion that the modified electrodes display charge-transport properties intermediate between typical diffusional and surface-bound couples.

Chronoamperometric studies were performed in order to measure the rates of charge propagation through the films. The results obtained in a series of studies are shown in Table II. Rates were measured by observing the current decay curve following a potential step past the one-electron wave for each complex within the polymeric film with 0.1 M $HClO_4$ in the external solution. Only the first 50 ms of each curve was used to avoid errors due to semiinfinite diffusion. The product of the diffusion coefficient for charge transfer and the concentration of redox sites, $D_{ct}^{1/2}C$, was obtained from the slopes of plots of current vs. $t^{-1/2}$. The surface coverage of redox sites within the films, Γ, was estimated by integration of the areas under cyclic voltammograms. Concentrations were calculated from Γ on the basis of the amount of polymeric material added to the electrode and with a film volume estimated by assuming a film density of 1.0 g/cm^3. Values of D_{ct} for the various complexes within the polystyrene sulfonate films were in the range 5×10^{-8}–1.2×10^{-8} cm^2 s^{-1}. They are faster by 1 order of magnitude than values obtained for $Ru(bpy)_3^{2+}$ in Nafion coatings.[22,23]

II. Catalytic Oxidation of Chloride to Chlorine. Figure 12 shows a rotated-disk voltammogram of an electrode modified with $[Ru(bpy)_2(H_2O)]_2O^{4+}$ (electrode I) in a solution containing 0.1 M LiCl at pH 1. Clearly, the modified electrode is a potent electrocatalyst for the oxidation of Cl^-. The catalytic current obtained is 2 orders of magnitude greater than that obtained at an unmodified glassy carbon electrode. Previous work has shown the Ru dimer to be an effective chloride oxidation catalyst in acidic solution when oxidizing equivalents are supplied either electrochemically at an electrode surface or chemically with Ce^{4+} as oxidant.[12]

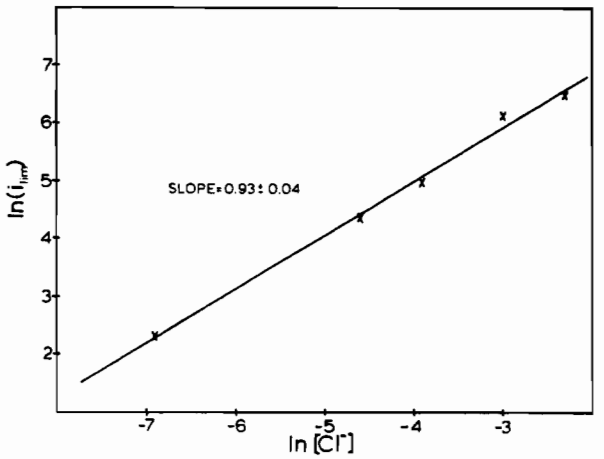

Figure 13. Plot of ln i_{lim} from rotated-disk voltammograms for electrode I vs. ln [Cl^-] in 0.10 M $HClO_4$; (ω = 1600 rpm; v = 10 mV/s).

Although the catalytic electrode is highly active, it is not very stable. If repeat voltammograms are recorded, the limiting current observed decreases by up to 10% for each scan. The reproducibility of the level of catalytic currents for different electrodes prepared in the same way was also disappointing (see Experimental Section). This fact coupled with the lack of stability under catalytic conditions made detailed studies of the electrocatalyzed process difficult, but with these limitations in mind, we have undertaken a number of mechanistic studies of the reaction.

The results of a series of rotated-disk voltammetry experiments are available. Due to the problems associated with reproducing electrodes, reliable, quantitative studies on the effects of changing the catalyst concentration within the film or of the film thickness have not been obtained. However, it has been observed that electrodes consisting of thicker films lead to greater catalytic activity than those with thinner films. A trend is observed that the amount of catalytic activity, i.e. catalytic current, increases with increasing total coverage (i.e. total moles of catalyst) regardless of whether the change in coverage arises from a higher loading percentage or thicker films.

The limiting current obtained has been found to be proportional to the concentration of Cl^- in the bulk solution. Figure 13 shows a plot of the natural log of the limiting catalytic current vs. ln [Cl^-] between 0.001 and 0.1 M. The plot is linear with a slope near unity (0.93 ± 0.04). The current values used take catalyst electroactivity in the absence of Cl^- as well as chloride electroactivity in the absence of catalyst into account. Background experiments in which Cl^- to Cl_2 oxidation was observed in the absence of catalyst showed no change in chloride electroactivity either with a bare glassy carbon electrode, with one coated with polymer in the same manner as for the modified electrodes, or with an electrode coated with a polymer containing the corresponding Os dimer, which displays no catalytic activity toward chloride oxidation in solution. The results obtained lead to the conclusion that chloride ion passes through the film in a facile manner and that the catalytic effect observed is, in fact, due to the presence of the dimer.

The effect of varying rotation rate in the RDE experiments was studied. Normal RDE experiments showed no systematic change in limiting currents with rotation rate, but a difficulty arises from degradation of the catalyst during an individual experiment. Catalyst degradation could affect the results by decreasing the current as progressive scans are made. Two experiments were performed to avoid this problem. First, the usual experiment was carried out twice with a differing direction of rotation rate progression (i.e. first increasing ω and then decreasing it). The experiment failed to reveal a dependence of i_{cat} on ω. The second test involved the use of a rotated-disk, pulse polarographic technique. The advantage sought in the experiment was the fact that in the pulse mode the electrode is at the potential for catalytic oxidation for only short periods. Since the electrode is relatively stable at potentials below those needed for catalysis, the technique

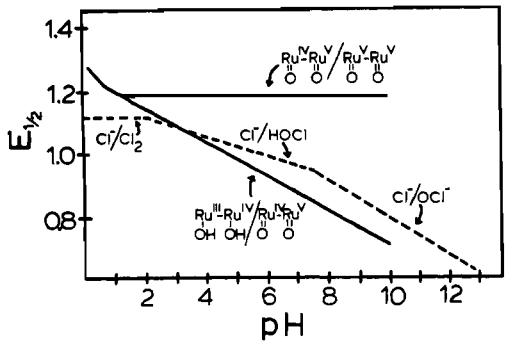

Figure 14. Plot of $E_{1/2}$ vs. pH for $[(bpy)_2Ru(H_2O)]_2O^{4+}$ [11,16a] and for the Cl_2/Cl^-–$HOCl/Cl^-$–OCL^-/Cl^- system.

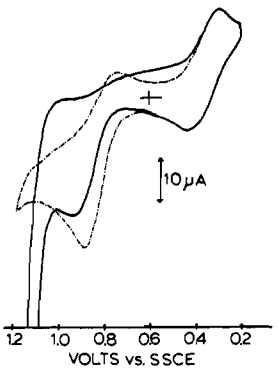

Figure 15. Cyclic voltammograms of electrode I, at pH 7, (- - -) without Cl^- present and (—) with 0.05 M Cl^- present in solution.

led to a substantial increase in the stability of the electrodes during the experiment. Test runs were performed to determine that repetitive scans led to little or no decrease in the limiting current obtained. Catalytic currents obtained in this manner showed no change with ω between 50 and 9300 rpm. Although there may be some dependence on ω at rotation rates lower than 50 rpm, it seems clear from this experiment as well as from those mentioned above that the catalytic currents obtained are not limited by mass transport of chloride ion to the electrode or by diffusion of chloride into the film.

Due to the strong pH dependences of the potentials of the various couples of the Ru dimer in solution and within the polymer matrix, we were interested in obtaining the pH dependence of the chloride oxidation catalysis. Figure 14 shows potential–pH diagrams for the dimer and Cl_2/Cl–$HOCl/Cl^-$–OCl^-/Cl^- couples.[16a] From the diagram, the dimer in its IV,V form is capable of catalyzing the oxidation of chloride to Cl_2 but only in solutions more acidic than pH 3.5. However, the IV,V/V,V couple (eq 7) is pH-independent and thermodynamically capable of oxidizing Cl^- at all pH values.

Figure 15 shows a cyclic voltammogram of electrode I in a solution buffered at pH 7 with added LiCl (solid line). Also shown is a cyclic voltammogram of the modified electrode in chloride-free solution at pH 7 (dashed line). That $(bpy)_2(O)Ru^VORu^V(O)(bpy)_2^{4+}$ is acting as the oxidized form of the catalyst is shown by the considerable catalytic current at this pH observed at potentials approaching 1.2 V. It is a very interesting point that it is not possible to observe this couple directly in the absence of Cl^- because the response for the couple is lost in the background. The fact that the onset of catalysis remains at the same potential without regard to pH supports the hypothesis that the active form is Ru(V)–Ru(V) and that the V,V/IV,V couple is pH-independent.

The degree of catalytic activity at higher pH values for the oxidized dimer is far less than that in more acidic solutions both in the film and in solution.[16a] Figure 16 shows a plot of catalytic limiting current from RDE experiments as a function of pH when the potential was scanned past the potential of the V,IV/V,V couple of the dimer. This decrease in catalytic activity upon increasing pH coupled with the fact that the Ru(V)–Ru(IV) form of the dimer is more accessible in basic solutions further implicates $[(bpy)_2(O)Ru^VORu^V(O)(bpy)_2]^{4+}$ as the active catalyst. The decrease in activity is associated with the accessibility of the Ru(V)–Ru(V) form of the dimer.

Controlled-potential electrolysis was performed to study the prolonged catalytic activity of the electrodes. A glassy carbon-disk electrode (geometric area 0.071 cm^2) modified with the dimer was held at a potential of 1.35 V in a pH 1 solution with 0.1 M NaCl and the resulting current vs. time curve recorded. An initial current density of 6.3 mA/cm^2 was obtained, which decayed with time ($t_{1/2}$ = 7.5 min). After 20 min 0.071 C had passed, which corresponded to the production of 3.68×10^{-7} mol of Cl_2, assuming that all of the catalytic current was due to Cl_2 production. The amount of electroactive catalyst on the electrode as determined by integration of a cyclic voltammetric wave was 1.36×10^{-10} mol. The electroactive catalytic sites, therefore, had turned over approximately 2700 times in this 20-min period, but their catalytic activity had fallen significantly as well. Repeating the experiment at higher $[Cl^-]$ (1.0 M NaCl) gave an initial current density of 100 mA/cm^2. The electrode, which contained 1.62×10^{-10} mol of catalyst, thus has an initial turnover rate of 225 mol of Cl_2/(mol of catalyst s). Under these conditions, however, the catalytic activity decays much more rapidly with a half-life for decomposition of 90 s and all catalytic activity had ceased after 10 min. At this stage 0.814 C had been passed, corresponding to 4.21×10^{-6} mol of Cl_2 or 26 000 mol of Cl_2/mol of catalyst. Although the catalytic electrode was deactivated at the end of the electrolysis, the electroactivity could be restored by resoaking in a solution of the dimer for 15 min as detailed below. In contrast, electrolysis of the same solution with a bare glassy carbon electrode of the same surface area passed 0.01 C in 20 min.

The use of dimer-containing electrodes produced with the Nafion ion-exchange membrane for electrocatalytic generation of chlorine was also studied. The Nafion films showed considerably less activity than the electrodes based on the poly(styrenesulfonate) polymer. Holding the Nafion electrodes at a potential of 1.40 V in a solution at pH 1 containing 1.0 M NaCl led to an initial current of 2.9 mA/cm^2, which decayed with $t_{1/2}$ = 8–10 min. This is far less than the 100 mA/cm^2 initial current found for the poly(styrenesulfonate) polymer under similar conditions and possibly indicative of slower charge transport within the Nafion membrane.

The use of the dimer-based electrode for larger scale catalytic production of Cl_2 was also studied. A coarse, reticulated, vitreous carbon electrode was immersed in a solution of *p*-chlorosulfonated polystyrene, removed, and dried in vacuo for 24 h. The electrode was subsequently soaked in a pH 9 solution containing the dimer for 1 h. The electrode was placed in an air-tight cell containing a solution of NaCl (0.1 M) at pH 1, and Ar was bubbled through the solution and subsequently through a solution containing 0.1 M NaOH to trap the Cl_2 produced as OCl^-. After electrolysis for 30 min at a potential of 1.40 V, 11.06 C were passed. The argon stream was continued for an additional 30 min and the Cl_2 that appeared in the trap analyzed for Cl_2 as OCl^- by iodometry. The titration gave 1.56×10^{-5} mol of OCl^-, which corresponded to a current efficiency (2 × mol of Cl_2/equiv of e^- passed) of 27% for Cl_2 production. The low efficiency is probably a consequence of the Cl_2 trapping scheme used, as well as the relatively crude cell design, which allows short circuiting by reaction of Cl_2 produced in the working compartment to pass through a frit and be reduced at the cathode. The same problems were also reported for Cl_2 production using the dimer system as a catalyst in solution.[12]

Catalyst Deactivation. The nature of the deactivation of the catalytic electrode was also investigated. The decay of catalytic current with time when the potential of the electrode was held at 1.40 V is not first order; i.e., a plot of ln *i* vs. time is nonlinear. Under these conditions the loss of catalytic activity appears not to be associated with loss of catalyst from the polymer film since, as noted earlier, the loss of catalyst from the film by leaching has a half-life of approximately 30 min. When solutions containing 0.1 M Cl^- are used, the catalytic current decays to 50% in a

considerably shorter period of time. With higher concentrations of chloride in the bulk solution the currents are greater but decay faster; as noted for 1.0 M Cl^- the current decays by 50% in only 90 s. From these observations it appears that the rate of decay of the electroactivity is related to the rate at which the electrocatalytic oxidation of Cl^- to Cl_2 occurs. The total number of catalytic turnovers increases with increasing rates of reaction, but the rate of catalyst deactivation also increases.

The cyclic voltammogram of the electrode after the catalytic current is essentially depleted shows a new wave with $E_{1/2} = 0.62$ V at a current level about 20% of the III,III/III,IV wave for the original complex. Cycling the electrode between 0.5 and 0.95 V for 30 min in a chloride-free solution partially restored the activity of the complex, but the total current was still less than 20% of the original. As mentioned earlier, soaking the electrode at this point for 15 min in a dimer-containing solution fully restores the electroactivity. An electrode can be used in a cycle of catalysis followed by regeneration by soaking in a dimer-containing solution with no loss of initial activity for three cycles.

The deactivation product seems to be an anated species as described for the electrode in a chloride-free solution. In aqueous solution loss of catalytic activity has been associated with formation of $(bpy)_2ClRuORu(H_2O)(bpy)_2^{3+}$ and $(bpy)_2ClRuORuCl(bpy)_2^{2+}$.[12a] The $E_{1/2}$ values for these complexes (at pH 1) in solution are 0.69 and 0.55 V, respectively, while the product in the film has $E_{1/2} = 0.62$ V. As a consequence, it seems reasonable to propose that the main product of catalyst deactivation may be a sulfonate complex with the complex covalently bound to the polymer. This is not surprising in light of the high concentration of sulfonate sites within the film. In this context it is important to recall the evidence suggesting that the Ru(V)–Ru(V) form of the dimer is the only, or at least by far the most active, form toward Cl^- oxidation. If oxidatively induced anation occurs giving $(bpy)_2XRuORu(H_2O)(bpy)_2^{3+}$ (X = Cl or $O_3SC_6H_4-$), access to Ru(V)–Ru(V) would be blocked since its appearance is contingent on the presence of bound H_2O and oxidative loss of protons to give oxo groups.

The observations described above and in earlier sections lead us to believe that the dimer is the intrinsic catalyst for the oxidation of Cl^- to Cl_2. This is an important point since RuO_2 is an excellent catalyst for the same reaction and the possibility exists that decomposition of the dimer or a related complex could lead to RuO_2 within the films. It is especially telling that the degree of catalytic behavior exhibited by the films decreases as the aqua dimer is replaced by its anated form and that hydrolysis returns the films to their active state.

The appearance of the oxidatively induced anation chemistry may be symptomatic of the underlying redox mechanism. In particular, steps involving Cl^- addition to an electrophilic oxygen

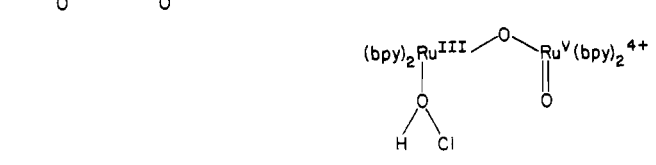

followed by dissociative loss of HOCl, could lead to a pathway for capture of the dimer by sulfonate binding.

With these thoughts in mind, the anation of the complex by chloride was studied within the film. If the modified electrode is cycled through the III,III/III,IV wave between 0.5 and 1.0 V for 30 min in a solution containing 0.1 M LiCl at pH 1, no evidence is obtained for any chemical change of the complex in the film. Holding the potential of the electrode at 0.5 or 1.0 V for 10 min gave the same result. It seems unavoidable that the dimer is stable with respect to anation in the Ru(III)–Ru(III) and Ru(III)–Ru(IV) forms, but upon reaching oxidation states as high as Ru(V)–Ru(V), anation must occur quickly and is perhaps coupled with the catalytic process or perhaps related to the loss of bpy from $M(bpy)_2(O)_2^{2+}$ (M = Ru, Os) and reflective

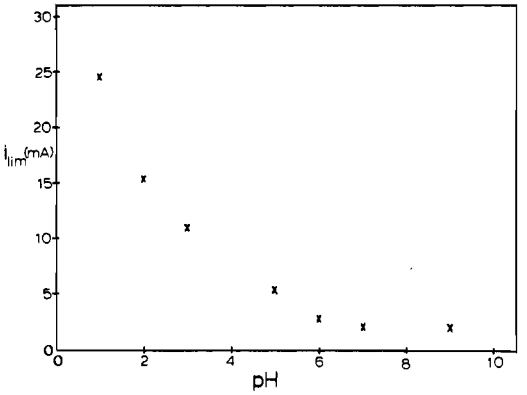

Figure 16. Plot of i_{lim} recorded at 1.4 V vs. SSCE from rotated-disk voltammograms for electrode I vs. pH (solutions contain 0.05 M LiCl; ω = 1600 rpm; v = 10 mV/s).

of a general lability toward ligand loss in the higher oxidation states.[25b,c]

Attempted Catalytic Oxidation of Water. The dimer has been shown to act as a catalyst for the oxidation of water to oxygen in solution,[9-11] but in the electrochemical data presented here, there is no evidence for the oxidation of water to oxygen. It should be noted that even in solution the time scale for water oxidation is seconds and is slow on the cyclic voltammetric time scale. We have attempted to discover the dimer-catalyzed oxidation of water to oxygen in the ion-exchange medium by utilizing bulk oxidation by Ce(IV) in the external solution with the dimer ion-exchanged into a Dowex cation-exchange resin. In the experiment approximately 30 mg of the dimer was ion-exchanged into approximately 100 mg of Dowex-X8 cation-exchange resin, and to the resulting dark blue-black beads was added excess Ce(IV) at pH 1 in an air-tight reaction vessel. Monitoring the gas above the reaction gave no evidence for O_2 production, as determined by gas chromatography. Under similar conditions O_2 production by the dimer is easily observable.

The environment in the Dowex resin is quite similar to that in the ion-exchange films used here in that it has both the same ion-exchange site and the same polymeric backbone, and it is significant that neither chemical nor electrochemical catalysis leads to dioxygen. Oxidation of chloride with the catalyst-loaded beads does occur. The same experiment performed in the presence of 0.1 M LiCl leads to facile Cl_2 production, as determined by iodometry.

Ratewise, there is a clear selectivity advantage for the oxidation of Cl^- over H_2O by the dimer even in solution. However, it is interesting to note that, in the environment of the polymeric film, the selectivity is enhanced to an even greater degree by seemingly the complete quenching of water oxidation. It will be interesting to discover if the rate advantage enjoyed by Cl^- will be maintained in competition with other substrates.

Catalysis of Chloride Oxidation by *cis*-$(bpy)_2Ru(H_2O)_2^{2+}$. It was reported earlier that the diaqua monomer *cis*-$(bpy)_2Ru(H_2O)_2^{2+}$ can be an effective catalyst for the oxidation of chloride to chlorine in acidic solution following oxidation to $(bpy)_2Ru(O)_2^{2+}$.[12a] An electrode containing the monomer was prepared by reduction of the Ru dimer as described above. Constant-potential electrolysis of this electrode at 1.35 V in a solution of 0.1 M $HClO_4$ containing 0.1 M NaCl gave an initial current density of 2.8 mA/cm^2, which decayed quickly ($t_{1/2}$ = 1 min) with all catalytic activity ceasing within 5 min. At this point 0.0355 C had been passed, corresponding to 140 mol of Cl_2/mol of catalyst. A cyclic voltammogram at this point showed no sign of the monomeric Ru(II)/Ru(III) couple. From these results and related observations it appears that the loss of activity can be traced to a more rapid leaching of the monomer from the film than for the dimer. This is an expected result given the lower charge type of the monomer.

Acknowledgments are made to the Army Research Office under Grant No. DAAG29-85-K-0121 and to the National Institutes

of Health under Grant No. 5-R01-GM32296-03 for support of this research.

Registry No. $[(bpy)_2Ru(H_2O)]_2O^{4+}$, 56110-87-3; $[(bpy)_2Ru(H_2O)]_2O^{5+}$, 96364-22-6; $(bpy)_2(H_2O)Ru^{III}ORu^{IV}(OH)(bpy)_2^{4+}$, 86045-59-2; *cis*-$(bpy)_2Ru(H_2O)^{2+}$, 72174-10-8; *cis*-$(bpy)_2Ru^{III}(H_2O)(OH)^{2+}$, 85027-43-6; $(bpy)_2(H_2O)RuORu(bpy)_2ORu(H_2O)(bpy)_2^{4+}$, 101695-59-4; $[(bpy)_2Os(H_2O)_2](ClO_4)_2$, 84988-26-1; *trans*-$(bpy)_2Ru(H_2O)^{2+}$, 72174-09-5; $[(bpy)_2Os(H_2O)]_2O^{4+}$, 99626-17-2; $(bpy)_2Ru(OH_2)ORu(OH)(bpy)_2^{3+}$, 100570-91-0; $[[(bpy)_2Os(H_2O)]_2O](ClO_4)_4$, 101695-60-7; $[[(bpy)_2Ru(H_2O)]_2O](ClO_4)_4$, 56110-88-4; $[(bpy)_2Ru(H_2O)_2](ClO_4)_2$, 16038-45-2; SnO_2, 18282-10-5; H_2O, 7732-18-5; Cl_2, 7782-50-5; Cl^-, 16887-00-6; C, 7440-44-0; O_2, 7782-44-7; Ru, 7440-18-8; Nafion, 39464-59-0.

Contribution from the Department of Chemistry, Purdue University, West Lafayette, Indiana 47907

Crystal and Molecular Structure of $[Ag(tmbp)_2]BF_4$. Origin of Flattening Distortions in d^{10} Complexes of the Type $M(NN)_2^+$

Kevin V. Goodwin, David R. McMillin,* and William R. Robinson*

Received October 31, 1985

The crystal and molecular structure of colorless bis(4,4',6,6'-tetramethyl-2,2'-bipyridyl)silver(I) tetrafluoroborate, $[Ag(tmbp)_2]BF_4$, has been determined and compared with those of Cu(I) complexes with analogous heteroaromatic, chelating ligands. The Cu(I) complexes are pseudotetrahedral, but they exhibit a characteristic flattening distortion, which results in a dihedral angle of 70–80° between the mean planes defined by the metal ion and each set of tmbp nitrogen atoms. The silver compound is found to be isomorphous and isostructural with $[Cu(tmpb)_2]ClO_4$. The dihedral ang'e defined above is 70.0 (1)° for the silver compound compared with 75.0° in the copper analogue. The fact that the dihedral angle in the Ag(I) complex is smaller than that in the Cu(I) complex tends to rule out the possibility that the flattening is due to an admixture of charge-transfer excited-state configurations in the ground state because the charge-transfer states are much less accessible in the Ag(I) system. The flattening is ascribed to a lattice effect that can be traced to stacking interactions involving the heteroaromatic ligands. The crystal system is orthorhombic, space group *Pbcn*, with $Z = 4$, $a = 16.737$ (2) Å, $b = 13.703$ (2) Å, $c = 11.916$ (2) Å, $V = 2733$ (1) Å^3, $R = 4.6\%$, and $R_w = 5.8\%$ for 1784 reflections.

Introduction

Heteroaromatic ligands such as 2,2'-bipyridine (bpy) and 1,10-phenanthroline and their derivatives, generically labeled as NN ligands, have long been used as reagents for the spectrophotometric determination of iron and copper.[1,2] The method is based on the intense visible absorbances of the Fe(II) and Cu(I) complexes, which have low-lying metal-to-ligand charge-transfer (CT) excited states.[3,4] Formally, the excitation involves the transfer of an electron from the d shell of the metal center to π^* orbitals of the coordinated ligands. Recently, a number of groups have begun to explore the photochemistry and photophysics of the CT states.[5-10]

Because of the d^{10} configuration, it was originally assumed that the $Cu(NN)_2^+$ systems would have a pseudotetrahedral coordination geometry with a dihedral angle of 90° between the mean planes of the respective ligands.[2] However, several structures of $Cu(NN)_2^+$ systems have shown that the complexes are flattened with dihedral angles typically between 70 and 80°.[11-17] Drew and co-workers observed a similar geometry in bis(2,2'-bi-4,5-dihydrothiazine)copper(I) tetraphenylborate, and they suggested that an admixture of the CT configuration into the ground-state wave function could explain the flattening,[18] since Cu(II) character

Table I. Experimental Crystallographic Data for $[Ag(C_{14}N_2H_{16})_2]BF_4$

formula	$AgC_{28}N_4H_{32}BF_4$
mol. wt	619.27
cryst dimens	0.3 × 0.3 × 0.15 mm
cryst syst	orthorhombic
space group	Pbcn (No. 60)
cell dimens[a]	$a = 16.737$ (2) Å, $b = 13.703$ (2) Å, $c = 11.916$ (2) Å, $V = 2733$ (1) Å^3, $Z = 4$, D(calcd) = 1.505 g/cm^3
radiation	Cu Kα (λ = 1.541 84 Å)
monochromator	graphite plate
θ range	3–56°
max scan time	60 s
scan angle	1 + 0.14(tan θ)
monitor reflecns	3 every 2 h; 2% nonsystematic variations
h,k,l limits	0–18,0–14,0–12
total no. of data	1784
no. of unique data	1784
no. of unique data with $F_o > 3\sigma(F_o)$	1255
no. of variables	221
μ(Cu Kα)	64.64 cm^{-1}
empirical abs cor	min trans, 79.7%; max, 99.9%; av, 94.5%
extinction	no cor necessary
$F(000)$	1264
residuals	R, 0.046; R_w, 0.058
wt	$1/(\sigma(F_o))^2 = 4F_o^2/\sigma(F_o^2)$; $\sigma(F_o^2) = [(\sigma(F_o))^2 + 0.05F_o^2]^{1/2}$

[a] From least-squares refinement of the setting of 25 carefully centered reflections in the range $15° < \theta < 23°$.

(1) Schilt, A. A. *Analytical Applications of 1,10-Phenanthroline and Related Compounds*; Pergamon: New York, 1969; pp 55–56.
(2) Welcher, F.; Boschmann, E. *Organic Reagents for Copper*; R. E. Krieger: Huntington, NY, 1979; p 242.
(3) Williams, R. J. P. *J. Chem. Soc.* **1955**, 137–145.
(4) Day, P.; Sanders, N. *J. Chem. Soc. A* **1967**, 1530–1536, 1536–1541.
(5) McMillin, D. R.; Gamache, R. E., Jr.; Kirchhoff, J. R.; Del Paggio, A. A. In *Copper Coordination Chemistry: Biochemical and Inorganic Perspectives in Copper Coordination Chemistry*; Adenine: Guilderland, NY, 1983; pp 223–235.
(6) McMillin, D. R.; Kirchhoff, J. R.; Goodwin, K. V. *Coord. Chem. Rev.* **1985**, *64*, 83–92.
(7) Kirchhoff, J. R.; Gamache, R. E., Jr.; Blaskie, M. W.; Del Paggio, A. A.; Lengel, R. F.; McMillin, D. R. *Inorg. Chem.* **1983**, *22*, 2380–2384.
(8) Edel, A.; Marnot, P. A.; Sauvage, J. P. *Nouv. J. Chim.* **1984**, *8*, 495–498.
(9) Creutz, C.; Chou, M.; Netzel, T. L.; Okumura, M.; Sutin, N. *J. Am. Chem. Soc.* **1980**, *102*, 1309–1319.
(10) Chum, H. L.; Koran, D.; Osteryoung, R. A. *J. Am. Chem. Soc.* **1978**, *100*, 310–312.
(11) Hämäläinen, R.; Turpeinen, U.; Ahlgren, M.; Raikas, T. *Finn. Chem. Lett.* **1978**, 199–202.
(12) Hämäläinen, R.; Turpeinen, U.; Ahlgren, M.; Raikas, T. *Cryst. Struct. Commun.* **1979**, *8*, 75–80.
(13) Dessy, G.; Fare, V.; *Cryst. Struct. Commun.* **1979**, *8*, 507–510.
(14) Burke, P. J.; McMillin, D. R.; Robinson, W. R. *Inorg. Chem.* **1980**, *19*, 1211–1214.
(15) Burke, P. J.; Henrick, K.; McMillin, D. R. *Inorg. Chem.* **1982**, *21*, 1881–1886.
(16) Hoffman, S. K.; Corvan, P. J.; Singh, P.; Sethulekshmi, C. N.; Metzger, R. M.; Hatfield, W. E. *J. Am. Chem. Soc.* **1983**, *105*, 4608–4617.
(17) Dobson, J. F.; Green, B. F.; Healy, P. C.; Kennard, C. H. L.; Pakawatchai, C.; White, A. H. *Aust. J. Chem.* **1984**, *37*, 649–659.

0020-1669/86/1325-2033$01.50/0